Supporting Information: Chromatic Aberration Correction for Atomic Resolution TEM Imaging from 20 kV to 80 kV

Martin Linck,* Peter Hartel, Stephan Uhlemann, Frank Kahl, Heiko Müller, Joachim Zach, and Max. Haider

Corrected Electron Optical Systems GmbH,

Englerstr. 28, D-69126 Heidelberg, Germany

Marcel Niestadt and Maarten Bischoff

FEI Company, Achtseweg Noord 5, 5651 GG Eindhoven, Netherlands

Johannes Biskupek, Zhongbo Lee, Tibor Lehnert, Felix Börrnert, Harald Rose, and Ute Kaiser

Central facility of electron microscopy, Ulm University,

Albert-Einstein-Allee 11, D-89081 Ulm, Germany

ABERRATION COEFFICIENTS OF THE 20 KV-SETTING

The aberration measurement was done by means of a tilt tableau with an outer tilt angle of 50 mrad. The object was an amorphous tungsten film of 2 nm thickness. Aberration coefficients are determined up to fifth axial and third off-axial order, respectively, corresponding to the phase plate shown in Figure 3(f) of the main publication. All non-circular axial aberrations up to including fifth order are zero within the 95%-confidence ranges of the measurement. For the aberration coefficients we use the definitions from [1]. The round aberrations C_3 and C_5 are adjusted such that a uniform PCTF beyond the 50 mrad aperture is established. The correction of the off-axial aberrations guarantees that this PCTF hardly changes within a considerable field of view. A transfer of 1000 equally well resolved image points can only be realized by correction of the off-axial coma, which is unavoidable for magnetic round lenses ($|B_{2G}| \approx 0.7$).

	Value	Angle	Confidence		Value	Angle	Confidence
A_2	5.65 nm	163.6°	19.9 nm	C_{1g}	2.7 nm/µm	-129.1°	6.3 nm/µm
B_2	11.1 nm	43.7°	17.3 nm	A_{1g}	3.3 nm/µm	162.1°	11 nm/µm
C_3	-12.9 µm	–	1.2 µm	A_{1G}	4.8 nm/µm	1.6°	11 nm/µm
A_3	279 nm	-43.1°	406 nm	A_{2g}	117 nm/µm	64.3°	143 nm/µm
S_3	146 nm	71.8°	363 nm	A_{2G}	23 nm/µm	51.6°	143 nm/µm
A_4	497 nm	160.8°	2.28 µm	B_{2g}	135 nm/µm	92°	126 nm/µm
D_4	1.16 µm	137.8°	1.4 µm	B_{2G}	50 nm/µm	135.4°	126 nm/µm
B_4	2.38 nm	-164.8°	2.65 µm				
C_5	3.96 mm	–	283 µm				
A_5	5.95 µm	156.1°	41.8 µm				
R_5	14.9 µm	-77°	25.4 µm				
S_5	2.93 µm	-41.3°	62.2 µm				

Table I. Measured coefficients of the axial and off-axial aberrations at 20kV.

RESOLUTION ESTIMATION

The estimation of the TEM information limit by means of Young's fringes is often seen very critical in that it generally yields too optimistic results. Thus, alternative methods have been suggested for a trustful estimation of the microscope's linear information transfer capabilities [2, 3].

Exemplarily, we have performed the so-called paraboloid method at 30 kV according to the work of Kimoto et al. [3]. A focus series of the 2 nm amorphous Tungsten sample was recorded to compare the linear information transfer to our Young's fringes results. Using a defocus step size of 1.81 nm, 64 images were recorded symmetrically around the Gaussian image plane (0.5 sec exposure time, 2048x2048 framesize, FEI CETA camera). Following the procedure in [3] the individual images were cross-correlated w.r.t. each other and Fourier transformed in all three dimensions. Subsequently, under identical conditions Young's fringes were acquired with an exposure time of 4.0 sec. Figure 1 shows that the resulting Ewald's sphere, i.e. the paraboloid of linear information transfer, basically reaches out as much as the visibility of Young's fringes. At this point, it should be emphasized that we do not use the 7 nm thick Germanium films as done in the publication of Kimoto et al. but only 2 nm thin amorphous Tungsten samples. The extreme thin Tungsten films serve excellent as weak phase objects even under low-voltage conditions. This can also be seen when comparing the non-linear contrast image contributions in the paraboloid method: In the publication of Kimoto et al. a significant non-linear image contrast can be found in the outer area of the paraboloid center plane; this contrast contribution is not present for our Tungsten samples. It should be noted that also the paraboloid method has its shortcomings in that the specimen degrades under the beam during focus series acquisition. Also it is very demanding to cross-correlate the images of the focus series with the desired accuracy as the transfer conditions and the object itself are changing throughout the series. Both effects will deteriorate the results of the paraboloid method.

An alternative method for assessment of the linear information limit had been presented by Barthel & Thust [2]. This approach, in fact, exactly corresponds to the tilt experiment that has been shown in Figure 4 of our manuscript (see [4]). The method of Barthel & Thust assumes that the information limit is determined by focus spread only; any other resolution-limiting effects, especially image spread, are not taken into account at all. If the incident
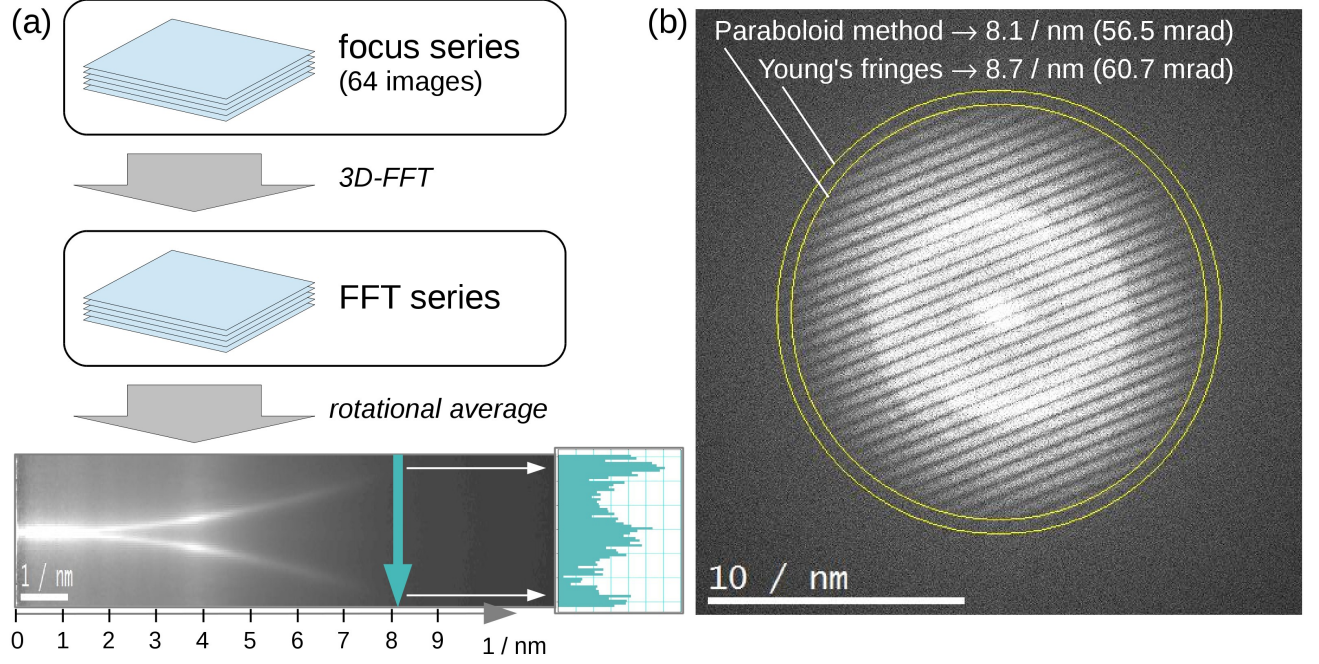
Figure 1. Comparison of the resolution assessment by Young's fringes and the paraboloid method at 30kV. (a) The 3D FFT of a through-focus series compresses linear phase contrast to a set of parabolic surfaces (Ewald's spheres). In the rotational average, this transfer reaches out to 8.1/nm. (b) The Young's fringes experiment evidently yields similar results.

electron beam is tilted w.r.t. the optic axis, a focus spread translates to a directly measureable, additional image spread. However, in the C_c/C_s-corrected instrument the tilt-induced image spread is small compared to the contribution from thermal magnetic field noise [5]. Therefore, the method of Barthel & Thust leads to an overestimation of the information limit: The determined focus spread of about 1 nm at 20 kV would yield an information limit of at least 74 mrad corresponding to 8.6 /nm, whereas we have shown only 62 mrad corresponding to 7.2 /nm (including image spread from thermal magnetic field noise).

In the work of Haider et al. [4] the dependence of non-linear image contrast on focus spread was investigated in great detail. By analyzing the general contrast formation in terms of the transmission cross coefficient it was shown how linear and non-linear contrast behave depending on the presence of focus spread. If focus spread is largely present (i.e. in C_c-uncorrected TEMs) the linear contrast contributions are strongly attenuated. Non-linear contrast partially remains present; this is especially true for scattering angles on the same achromatic circle: the correspondingly resulting non-linear contrast contributions are

not dampened by chromatic aberrations at all. In fact, this is the dominating reason that Young's fringes generally strongly overestimate linear information transfer. However, if no focus spread is present (C_c corrected), the non-linear contrast transfer is not "preferred" over linear contrast any more. Therefore, the Young's fringes experiment in fact can yield reliable resolution estimates, however, only if applied under these special conditions (C_c-corrected and suitable sample). Moreover, in the case of an image-spread-limited microscope resolution, the linear and non-linear terms of contrast formation are equally affected by the image spread damping envelope. Thus, C_c-corrected microscopes will intrinsically provide a much smaller resolution mismatch in-between the images of weak-phase objects and strongly scattering crystalline materials.

IMAGE PROCESSING

The signal-to-noise ratio caused by the limited electron dose can be enhanced by post-processing the recorded low dose images by a self-averaging algorithm. In this algorithm, the lattice is shifted into different directions in order to match the nearby neighbors and an average of all the shifted images is obtained. This method is equivalent to increasing the electron dose indirectly and can be effectively applied for defect-free regions of the graphene and MoS_2 images.

SUPPLEMENTAL MOVIE S1: TIME DEVELOPMENT OF AD-ATOMS EMBEDDED INTO A VACANCY WITHIN THE GRAPHENE LATTICE

The movie S1 shows the time development of single foreign atoms (presumably Si atoms as contamination from sample preparation) trapped in a vacancy of the graphene lattice. While the ad-atoms move within the graphene vacancy, the vacancy itself does not grow at all. The focus conditions were set to overfocus to show white atom contrast. The exposure time for each frame is 1 s and a dose rate of 2.5 $e^-/nm^2/s$. The raw images were aligned and corrected for drift. No additional filtering or image enhancement was applied. The series is speeded up by factor 50 leading to a frame rate of 0.2 fps. The defect does not grow on a time scale of 5 min of continuous irradiation at 30 kV; only the foreign atoms change their position in contrary to similar experiments at higher voltages such as 80 kV.

* linck@ceos-gmbh.de

[1] H. Müller, I. Maßmann, S. Uhlemann, P. Hartel, J. Zach, and M. Haider, Nuclear Instruments and Methods in Physics Research Section A: Accelerators, Spectrometers, Detectors and Associated Equipment **645**, 20 (2011).

[2] J. Barthel and A. Thust, Phys. Rev. Lett. **101**, 200801 (2008).

[3] K. Kimoto, K. Kurashima, T. Nagai, M. Ohwada, and K. Ishizuka, Ultramicroscopy **121**, 31 (2012).

[4] M. Haider, P. Hartel, H. Müller, S. Uhlemann, and J. Zach, Microscopy and Microanalysis **16**, 393 (2010).

[5] S. Uhlemann, H. Müller, P. Hartel, J. Zach, and M. Haider, Physical review letters **111**, 046101 (2013).